*Proc. Natl. Acad. Sci. USA*
Vol. 75, No. 4, pp. 1727–1730, April 1978
Biochemistry

# Kinetics of biphasic reconstitution of tobacco mosaic virus *in vitro*

(virus encapsidation/RNA–protein interaction)

MEGUMI FUKUDA*, TAKESHI OHNO*, YOSHIMI OKADA*, YOSHIAKI OTSUKI†, AND ITARU TAKEBE†

* Department of Biophysics and Biochemistry, Faculty of Science, University of Tokyo, Tokyo 113, Japan; and † Institute for Plant Virus Research, Tsukuba Science City, Yatabe, Ibaraki 300-21, Japan

*Communicated by Heinz Fraenkel-Conrat, January 30, 1978*

ABSTRACT **The kinetics of the *in vitro* reconstitution of tobacco mosaic virus from its RNA and protein were studied by measuring the increase in turbidity, the development of ribonuclease-resistant infectivity, the encapsidation of the terminal ends of the RNA, and the growth of rod length. The results showed that the reconstitution reaction consists of two processes in which the direction, timing, and rate of assembly are different. Rapid elongation of particles toward the 5′ end of the RNA proceeds in the first 5–7 min to give intermediate particles of 260 nm in length in which only the 5′ terminus of the RNA is encapsidated. The subsequent process requires 30–50 min, is accompanied by a slow increase in turbidity, and gives rise to rods of the full length, 300 nm. The 3′ terminus becomes RNase resistant by this process with concomitant development of ribonuclease-resistant infectivity, showing that the 3′-distal portion of the RNA is encapsidated in the direction of 5′ to 3′. The rate of rod elongation by the second process is less than 1/10 of that by the first process.**

The reconstituon of tobacco mosaic virus (TMV) had been thought for some years to start at the 5′ terminus of the viral RNA and to elongate unidirectionally (1–4). However, since the 5′ terminus of TMV RNA was found to be capped with a 7-methylguanosine moiety (5, 6), numerous experiments have been done to reevaluate the earlier proposed assembly mechanism. Recently, several laboratories independently reached the conclusion that reconstitution starts at an internal region of the RNA, about 800–1000 nucleotides from the 3′ terminus, and that the elongation occurs bidirectionally (7–10). In an early phase of the reaction, the rod elongation toward the 5′ end is much favored over that toward the 3′ end (9–11).

The present study deals with kinetics of the bidirectional elongation of TMV rods during the reconstitution reaction, studied by measuring turbidity, infectivity, RNase resistance of the two ends of RNA, and rod length. The results show that reconstitution takes place in two successive phases that differ not only in the direction, but also in the rate of rod elongation. Rods with a length of 260 nm were identified as the product of the early process of reconstitution.

## MATERIALS AND METHODS

**Preparation of TMV, TMV Protein, TMV RNA, and Tritium-Labeled TMV RNA.** TMV, a Japanese common strain OM, was purified by polyethylene glycol precipitation (12) followed by differential centrifugation. TMV protein and RNA were isolated by the acetic acid method (13) and by phenol-bentonite extraction (14), respectively. TMV RNA radioactively labeled at its termini was prepared by periodate oxidation and subsequent reduction with tritiated sodium borohydride (8). Both the 5′- and the 3′-ribosyl ends of TMV RNA were labeled with about the same efficiency.

The costs of publication of this article were defrayed in part by the payment of page charges. This article must therefore be hereby marked "*advertisement*" in accordance with 18 U. S. C. §1734 solely to indicate this fact.

**Reconstitution Reaction.** A protein disk preparation was obtained by incubation of the protein (6.6 mg/ml) for 24 hr in 0.1 M phosphate buffer (pH 7.0) at 20°. Reconstitution reactions were carried out in the same buffer at 20° by mixing the protein disk preparation (5.6 mg/ml) with a mixture of TMV RNA (0.13 mg/ml) and tritium-labeled TMV RNA (0.05 mg/ml). At intervals, aliquots were withdrawn to determine the rod lengths, the ribonuclease resistance of tritium-labeled termini, and the infectivity.

**Turbidimetric Measurement during Reconstitution Reaction.** The reconstitution reaction during the initial 90 min of the reaction was followed by the increase in absorbance at 310 nm with a Gilford model 250 spectrophotometer.

**Rod Length Measurements by Electron Microscopy.** An aliquot from the reaction mixture was diluted 1:100 with ice-cold 0.01% (wt/vol) bovine serum albumin solution, and minute drops of the mixture were placed on carbon-coated electron microscope grids. The grids were immediately transferred to a desiccator and kept under reduced pressure overnight. The specimens were then negatively stained with 1% (wt/vol) phosphotungstic acid containing 0.15% (wt/vol) Driwell (Fuji Photofilm Co. Ltd.), and were photographed at a nominal magnification of 20,000 × with a Hitachi H 500 electron microscope. The exact magnification was determined with a standard TMV preparation. The negative plates were further magnified by 10 × using a shadowgraph to measure the length of virus rods. The rods were classified into 30 length classes, each spanning 10 nm.

**Analysis of RNase Resistance of Tritium-Labeled Termini.** Aliquots from the reconstitution mixture were treated with RNase A (0.2 μg/ml) at 25° for 30 min and were then centrifuged at 24,000 rpm for 2 hr on 5–20% sucrose gradients in 10 mM phosphate buffer (pH 7.2) in an RPS-25 swinging bucket rotor (Hitachi). After centrifugation, the gradients were fractionated and the absorbance and radioactivity of each fraction were measured. The sedimentable particle fractions containing radioactivity were collected and virus was precipitated with trichloroacetic acid (10%). The precipitates were dissolved in 0.3 M KOH and were kept at 37° for 18 hr. Tritium-labeled terminal nucleoside trialcohols of particle fractions were analyzed by phosphocellulose column chromatography as described (8, 15).

**Infectivity Assay.** Aliquots of the reaction mixture were treated with RNase and centrifuged on sucrose gradients as described above. Fractions of sedimentable particles were collected, diluted appropriately with 0.1 M phosphate buffer (pH 7.0), and inoculated on nine half-leaves of *Nicotiana tabacum* L. cv. Xanthi nc. A solution of TMV (0.05 μg/ml) inoculated on the opposite half-leaves served as a standard; infectivity of samples was expressed as relative lesion number,

Abbreviation: TMV, tobacco mosaic virus.

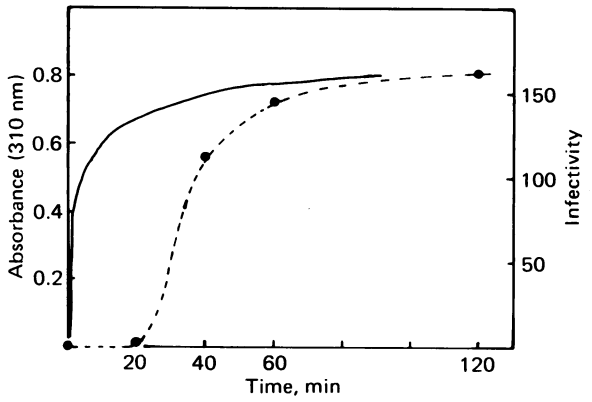


FIG. 1. Time course for the reconstitution of TMV measured by turbidimetry and infectivity. Reconstitution was performed by adding a mixture of tritiated and unlabeled RNA (0.05 and 0.13 mg/ml, respectively) to a protein disk preparation (5.58 mg/ml), in 0.1 M phosphate buffer (pH 7.0), at 20°, and was followed by measuring the increases in the absorbance at 310 nm (—) and in the RNase-resistant infectivity (●- - -●).

with the number of lesions produced by the standard TMV as 100.

## RESULTS

**Development of Turbidity and RNase-Resistant Infectivity.** As shown in Fig. 1, the turbidity of the reaction mixture increased very rapidly during the first few minutes but only gradually thereafter. However, the turbidity continued to increase even after 30 min, though at a low rate. Development of RNase-resistant infectivity during the reconstitution reaction followed a time course quite different from that of the turbidity increase (Fig. 1). RNase-resistant infectivity appeared only after a time lag of about 20 min and increased to a near maximal level during the next 40 min, as previously reported by Okada and Ohno (4). This indicated that the initial rapid rise of turbidity is not due to the formation of complete TMV particles, contrary to the previous conclusion by Butler and Klug (1) and by Butler (16). They interpreted the initial rise of turbidity to represent the production of full-length TMV rods and estimated the time for full reconstitution as 6.5 min. In the experiment of Fig. 1, the specific infectivity of the rods reconstituted for 2 hr was 57% of that of standard TMV. Taking into account the presence of rods reconstituted from noninfectious $^3$H-labeled RNA, this indicates that the infectivity of viral RNA was largely retained during the reconstitution reaction.

**Encapsidation of RNA Termini.** In order to determine the timing of encapsidation of the 5′ and the 3′ termini of TMV RNA, aliquots were withdrawn at intervals during reconstitution, treated with RNase, and analyzed by sucrose gradient centrifugation. Fig. 2 shows some of the sedimentation profiles of RNase-treated rods from the reconstitution mixture. The encapsidated portion of the viral RNA thus recovered as sedimentable rods was then hydrolyzed and chromatographed to see which terminus it contained (Table 1). At 5 min (Fig. 2*A*), a large amount of sedimentable rods was already formed, but these had only a trace amount of radioactivity. This shows that neither terminus of the growing rods was coated in an early stage of the reconstitution process, confirming the previous report by Ohno *et al.* (8). The sedimentable particles at 5 min consist therefore mainly of incompletely reconstituted particles having both 5′ and 3′ RNA tails, such as observed by Lebeurier *et al.* (10).

Fig. 2*B* shows the sedimentation profile of rods 20 min after

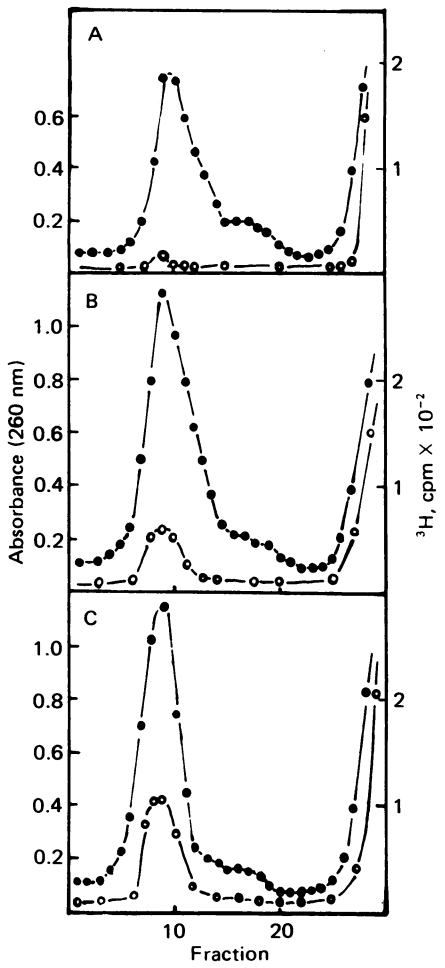


FIG. 2. Sedimentation profiles of reconstituted particles after RNase treatment. Reconstitution mixture was the same as that of Fig. 1. After 5 min (*A*), 20 min (*B*), and 2 hr (*C*) of incubation, an aliquot of the reaction mixture was treated with RNase A (0.2 μg/ml) at 25° for 30 min and centrifuged on 5–20% sucrose gradients. Sedimentation was from right to left. ●, Absorbance at 260 nm; ○, radioactivity.

initiation of the reconstitution reaction. These particles contained RNase-resistant radioactivity, which was identified as a derivative of m$^7$GpppGp from the 5′ end of the RNA (Table 1). Little radioactivity was recovered from the 3′ end of the RNA. The population of particles at 20 min is therefore believed to be mainly rods having only the 3′ tail of the RNA at one end.

When formation of virus particles was completed after 2 hr of incubation, the particle fractions (Fig. 2*C*) contained the radioactivity from both the 5′ and the 3′ ends of the RNA in equal amounts (Table 1). These results constitute good evidence that the reconstitution starts at an internal region of the RNA

Table 1. Recovery of $^3$H-labeled RNA termini in reconstituted particles

| Time after initiation, min | Radioactivity, cpm | | |
|---|---|---|---|
| | 5′ End | 3′ End | 3′ End/5′ end |
| 5 | 184 | 3 | 0.02 |
| 20 | 446 | 9 | 0.02 |
| 40 | 615 | 254 | 0.41 |
| 60 | 575 | 535 | 0.91 |
| 120 | 792 | 780 | 0.99 |

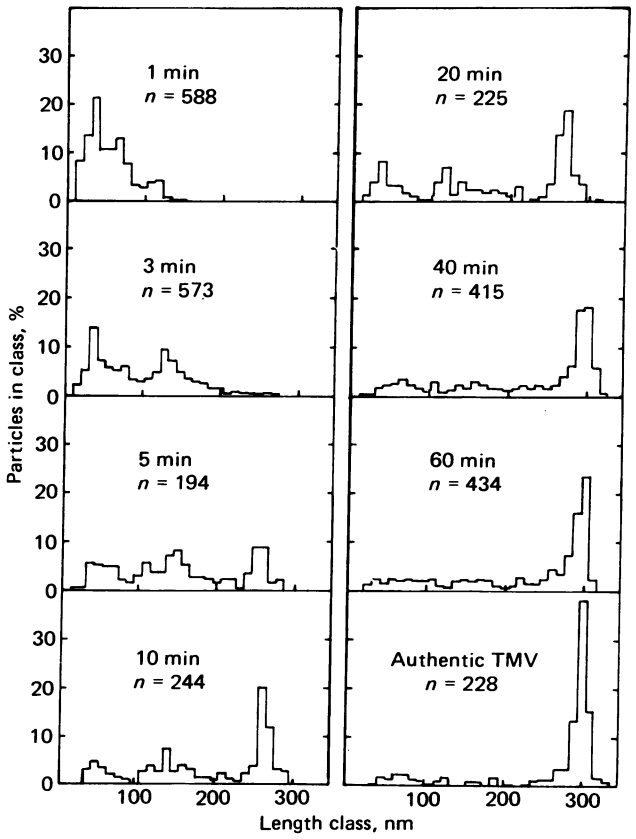


FIG. 3. Histograms of length distributions of growing rods and authentic TMV, from measurements by electron microscopy after negative staining with phosphotungstic acid. Reconstitution mixture was the same as that of Fig. 1. Time after initiation of reconstitution and total number of particles measured ($n$) are shown for each histogram.

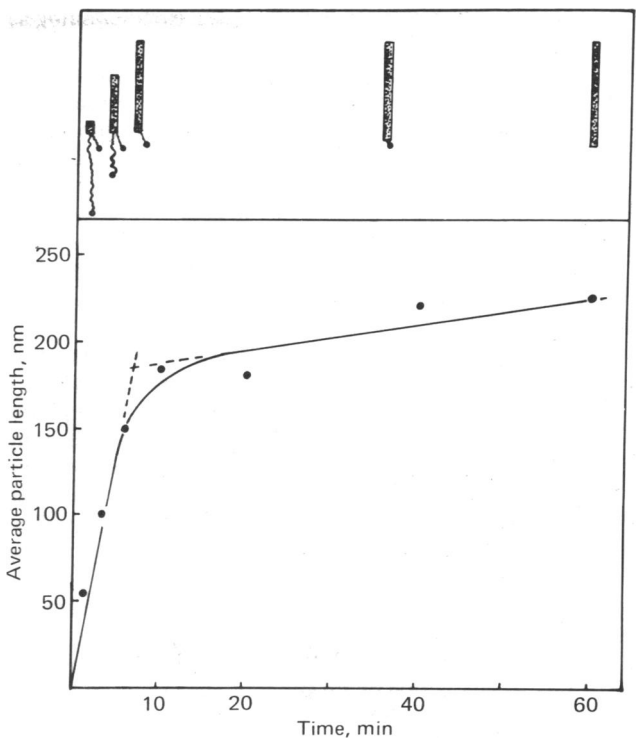


FIG. 4. Growth of average rod lengths during reconstitution of TMV. (*Lower*) Number-average particle lengths at each indicated time were calculated from the results in Fig. 3. (*Upper*) Schematic representation of the structures of growing rods during the reconstitution process. Open and solid symbols represent the 5′ and the 3′ ends of TMV RNA, respectively.

and proceeds first toward the 5′ terminus and that of the 3′ terminus becomes encapsidated much later. Encapsidation of the 3′ end of the RNA parallels the appearance of the RNase-resistant infectivity (Fig. 1).

**Growth of Rod Length.** Fig. 3 summarizes the length distribution of reconstituted rods at various times of reaction as determined by electron microscopy. The first appearance of particles with a length of around 260 nm was at about 5 min after initiation of the reconstitution reaction. The elongation of rods beyond this length apparently stopped for about 15 min, since even at 20 min the 260-nm particles still predominated in the histogram.

In our previous paper (9), we demonstrated that reconstitution starts at an internal region about 39 nm from the 3′ end of TMV rods and that the initiation is followed by encapsidation of the 5′-distal portion of TMV RNA. The length of rods should, therefore, be about 260 nm when the 5′ terminus of the RNA is encapsidated. The time course of the encapsidation of the 5′ end of the RNA (Table 1) is also in good agreement with the appearance of 260-nm particles. These results indicate that the initial rapid elongation toward the 5′ end of the RNA gives 260-nm particles when the 5′ end of the RNA is encapsidated.

At 40 min after initiation of the reaction, a number of full-length particles were detected. This is the time at which infectivity appears (Fig. 1) and the 3′ end of the RNA becomes RNase resistant (Table 1).

In order to see the kinetics of rod growth more clearly, the number-average rod length was plotted against time (Fig. 4). During the reconstitution reaction, rod elongation occurs initially at a high rate for about 5–7 min and subsequently at a low rate for about 30–50 min until rods reach an average length of about 230 nm. The average length of a purified TMV preparation was about 260 nm. The shorter average length of reconstituted particles is apparently due to the presence of some shorter RNA pieces in the reconstitution mixture.

## DISCUSSION

The evidence presented in this paper indicates that the elongation of growing TMV rods consists of two processes different in direction, in timing, and in rate of growth. The rapid elongation in the first 5–7 min gives intermediate particles 260 nm long (Fig. 3) in which only the 5′ end of the RNA is encapsidated. The length of 260 nm is in accordance with that of the distance between the initiation site of reconstitution and the 5′-terminal end of the RNA. Once the 5′ terminus of the RNA is encapsidated, reconstitution occurs slowly toward the 3′ end (Fig. 4). The rate of elongation toward the 3′ end appears to be less than $1/10$ that of elongation toward the 5′ end. When the 3′ terminus is encapsidated, the reconstitution reaction is complete and an infective virus particle is formed (Figs. 1 and 4 and Table 1). A simplified schematic representation of the structure of growing rods is given in Fig. 4.

Butler and Klug (17) and Butler and Finch (18) previously determined the length distribution of growing rods during reconstitution of TMV. Their observations differ from our results in that they did not notice the presence of 260-nm rods as an intermediary product and that 300-nm, full-length rods appeared as early as 5 min after the start of the reaction. The apparent discrepancies may be explained by the fact that they

classified rods into only seven length classes, each spanning as long as 40 nm. Since the class of longest rods included those rods 260–300 nm long, it is not surprising that these workers failed to detect the accumulation of 260-nm rods and erroneously concluded that some full-length rods are formed within 5 min. The formation of full-length rods was never checked in their experiments by the infectivity assay. In addition, the presence in their RNA preparations of broken molecules in rather large amounts makes their data less reliable. The reconstituted rods of Butler and Finch (18) thus had an average length as small as 140 nm and the proportion of rods in the 260 to 300-nm length class was only 10%.

A structural model for the rods during the rapid elongation was proposed by Lebeurier *et al.* (10) and by Butler *et al.* (11). In this model, the 5′ tail of the RNA threads back through the central channel of the rod. As the rod grows, the 5′ tail feeds up through the tube. Evidence has been presented that the rapid elongation proceeds by stepwise additon of proteins as individual subunits or as smaller aggregates (4, 19, 20). An alternative possibility that coat protein is added to the growing top of rods as preformed, 20S two-ring disks (1, 18, 21) seems improbable because of its topological complexity. The rate of elongation toward the 3′ end appears to be less than $1/10$ that of elongation toward the 5′ end (Fig. 4). Such a marked difference in the rate of elongation could probably be accounted for by the configuration of the RNA in growing rods or by the polarity of the protein structure.

It seems to be reasonable to assume that assembly of TMV *in vivo* follows a course basically similar to that found for its reconstitution *in vitro*, though there is no definite evidence for this assumption. One might speculate then what the biological significance of the bidirectional encapsidation may be. It is known that a short piece of RNA containing the 3′-terminal 750 nucleotides of TMV RNA occurs in infected tissues and that this RNA functions as messenger of coat protein in the wheat germ cell-free systems (22, 23). Lebeurier *et al.* (10) hypothesized that this RNA may be produced by replication of the free 3′ tail of the RNA of incompletely assembled virus. If this hypothesis is correct, the slow encapsidation of the 3′-distal portion of TMV RNA makes sense, since it keeps the 3′ tail of the RNA uncoated for a longer time and thus allows the preferential production of coat protein messenger RNA. Full elucidation of the detailed mechanisms and the biological meaning of the bidirectional, rapid and slow, elongation must await further experimentation.

This work was supported in part by a Grant-in-Aid for Scientific Research from the Ministry of Education, Science and Culture, Japan and a grant from the Toray Science Foundation.

1. Butler, P. J. G. & Klug, A. (1971) *Nature New Biol.* **229**, 47–50.
2. Ohno, T., Nozu, Y. & Okada, Y. (1971) *Virology* **44**, 510–516.
3. Thouvenel, J. C., Guilley, H., Stussi, C. & Hirth, L. (1971) *FEBS Lett.* **16**, 204–206.
4. Okada, Y. & Ohno, T. (1972) *Mol. Gen.Genet.* **114**, 205–213.
5. Zimmern, D. (1975) *Nucleic Acids Res.* **2**, 1189–1201.
6. Keith, J. & Fraenkel-Conrat, H. (1975) *FEBS Lett.* **57**, 31–33.
7. Zimmern, D. & Wilson, T. M. A. (1976) *FEBS Lett.* **71**, 294–298.
8. Ohno, T., Sumita, M. & Okada, Y. (1977) *Virology* **78**, 407–414.
9. Otsuki, Y., Takebe, I., Ohno, T., Fukuda, M. & Okada, Y. (1977) *Proc. Natl. Acad. Sci. USA* **74**, 1913–1917.
10. Lebeurier, G., Nicolaieff, A. & Richards, K. E. (1977) *Proc. Natl. Acad. Sci. USA* **74**, 149–153.
11. Butler, P. J. G., Finch, J. T. & Zimmern, D. (1977) *Nature* **265**, 217–219.
12. Leberman, R. (1966) *Virology* **30**, 341–347.
13. Fraenkel-Conrat, H. (1957) *Virology* **4**, 1–4.
14. Fraenkel-Conrat, H., Singer, B. & Tsugita, A. (1961) *Virology*, **14**, 54–58.
15. Ohno, T. & Okada, Y. (1977) *Virology* **76**, 429–532.
16. Butler, P. J. G. (1972) *J. Mol. Biol.* **72**, 25–35.
17. Butler, P. J. G. & Klug, A. (1972) *Proc. Natl. Acad. Sci. USA* **69**, 2950–2953.
18. Butler, P. J. G. & Finch, J. T. (1973) *J. Mol. Biol.* **78**, 637–649.
19. Ohno, T., Takahashi, M. & Okada, Y. (1977) *Proc. Natl. Acad. Sci. USA* **74**, 552–555.
20. Richards, K. E. & Williams, R. C. (1973) *Biochemistry* **12**, 4574–4581.
21. Butler, P. J. G. (1974) *J. Mol. Biol.* **82**, 333–341.
22. Hunter, T. R., Hunt, T., Knowland, J. & Zimmern, D. (1976) *Nature* **260**, 759–764.
23. Siegel, A., Hari, V., Montgomery, I. & Kolcz, K. (1976) *Virology* **73**, 363–371.